

Transition to Tumbling and Two Regimes of Tumbling Motion of a Vesicle in Shear Flow

Vasily Kantsler and Victor Steinberg

Department of Physics of Complex Systems, Weizmann Institute of Science, Rehovot, 76100 Israel

(Received 4 October 2005; published 24 January 2006)

Experimental results on the tank-treading-tumbling transition in the dynamics of a vesicle subjected to a shear flow as a function of a vesicle excess area, viscosity contrast, and the normalized shear rate are presented. Good agreement on the transition curve and scaling behavior with theory and numerical simulations was found. A new type of unsteady motion at a large degree of vesicle deformability was discovered and described as follows: a vesicle trembles around the flow direction, while the vesicle shape strongly oscillates.

DOI: 10.1103/PhysRevLett.96.036001

PACS numbers: 83.50.-v, 87.16.Dg, 87.17.Jj

The dynamics of individual vesicles under nonequilibrium conditions has received increasing attention in recent years in theory [1–3], numerical simulations [4–6], as well as in experiments [7–10]. This interest is motivated, first, by the strong resemblance in dynamical behavior of real biological cells, and second, by a possibility to understand rheological properties of vesicle solution flows.

A vesicle is a liquid droplet bounded by a closed phospholipid bilayer membrane (usually unilamellar) suspended in a fluid that can be either the same solvent as an inner one or different. Both the volume and the surface area of the vesicle are conserved. The former means that the vesicle membrane is considered to be impermeable, at least on the time scale of the experiment, and the latter means that the membrane dilatation is neglected [1–3].

It is known that vesicles in a shear flow reveal two types of motion, tank-treading and tumbling, and a range of existence of each of them depends on two main control parameters: the excess area (dimensionless), $\Delta = S/R^2 - 4\pi$, and the viscosity contrast, $\epsilon = \eta_{\text{in}}/\eta_{\text{out}}$. Here R is the effective vesicle radius related to its volume via $V = \frac{4}{3}\pi R^3$, S is the vesicle surface area that exceeds that of a sphere with the same volume by Δ , η_{in} and η_{out} are the dynamic viscosities of inner and outer fluids, respectively. At sufficiently low $\epsilon < \epsilon_c(\Delta)$, a steady mean vesicle orientation angle with respect to the shear flow direction and a tank-treading membrane motion are found [1,2,8,10], whereas at $\epsilon > \epsilon_c(\Delta)$ according to theoretical predictions [1,3], a transition to a tumbling motion should occur, when a vesicle axis rotates with respect to the flow direction. This transition is of fundamental importance, since it should alter rheological properties of a vesicle solution by reducing dissipation [3,6,11].

In this Letter we report first experimental studies of the tank-treading-tumbling transition in a shear flow as a function of the excess area and the viscosity contrast. We also present results on two different types of tumbling motion characterized by different dimensionless shear rate, $\chi = \dot{\gamma}\eta_{\text{out}}R^3/\kappa$, that determines the degree of vesicle deformability under the shear rate, $\dot{\gamma}$. Here κ is the bending rigidity of the membrane.

There were numerous attempts to theoretically describe both types of the vesicle motion and the transition between them, particularly in regards to the dynamics of red blood cells in a shear flow. Keller and Skalak [1], by making a bold assumption about a fixed ellipsoidal shape of a vesicle with a moving membrane and by neglecting thermal fluctuations, have suggested theory that provides amazingly accurate description of the vesicle dynamics in both regimes of motion and particularly of the transition to tumbling. They derived a generic evolution equation for the vesicle inclination angle, ϕ , in a form [1]:

$$\dot{\gamma}^{-1} \frac{d\phi}{dt} = A + B(\Delta, \epsilon) \cos(2\phi), \quad (1)$$

where $A = -1/2$ and $B(\Delta, \epsilon)$ is a function defined by a model. However, one gets two regimes and scaling in the transition region without going into details of a specific model. The steady solution for ϕ exists and is defined by $\cos(2\phi) = -A/B$ only if $|A/B| < 1$. Otherwise, no steady state solution exists, and a vesicle tumbles in a shear flow [1,3]. The value $|A/B| = 1$ corresponds to $\phi = 0$, the transition value to tumbling. For a rigid body, as found long time ago in Ref. [12], one has $|A/B| > 1$; i.e., tumbling occurs always without a threshold. In a general case, when a tank-treading motion is taken into account, the ratio $|A/B|$ is a function of Δ and ϵ , and it can be larger or smaller than unity. According to Ref. [1], the tumbling occurs at $\epsilon \geq \epsilon_c(\Delta)$, where $\epsilon_c(\Delta)$ is determined by $|A/B| = 1$. At $\epsilon < \epsilon_c$ and close to the transition the steady solution shows scaling $\phi \propto \sqrt{\epsilon_c - \epsilon}$ [1,5], where $\phi = 0$ is the threshold value. At $\epsilon > \epsilon_c$ the transition via a saddle-node bifurcation to tumbling occurs [1,3,5]. It is remarkable that both the more intricate theory [5] that considers a vesicle as a deformable object, which shape is not given *a priori* but is obtained as a result of an interplay between flow, bending rigidity, and the physical constraints, and the numerical simulations [6] based on the deformable vesicle model show rather close agreement with Ref. [1]. Very recently further refinement of the Keller-Skalak theory that considers also morphological changes, was suggested [11]. This phenomenological model consists of two coupled

equations; one of them is Eq. (1) and another is for a vesicle deformation. As a result, the vesicle shape has time dependence similar to that of the angular velocity [11].

Measurements of the vesicle dynamics were conducted in a near-wall shear flow at a half height of a microchannel via epifluorescent microscopy. The rectangular channel with $380 \mu\text{m}$ height and $250 \mu\text{m}$ width was manufactured in silicone elastomer by soft lithography [13]. An observation area $87 \times 66 \mu\text{m}^2$ was captured by Mintron MTV-12V1 CCD camera and digitized via Ellips Rio frame grabber. A mechanical chopper, synchronized with CCD camera and installed in the Ar-ion laser beam path, reduced actual exposure time down to $\sim 1 \text{ m sec}$. It allowed to capture vesicles with velocity up to hundreds $\mu\text{m}/\text{sec}$ without noticeable smearing of a vesicle image. The microchannel can be translated in the direction of the flow. Image processing and control of stepping motor drivers were performed under MATLAB.

Vesicles were prepared by electroformation method [14]. The lipid solution, consisted of 85% dioleoylphosphatidylcholine (DOPC, Sigma) and 15% fluorescent phosphatidylcholine (PC) (molecular probes) dissolved in 9:1 v/v chloroform-methanol solvent, was used. As an inner fluid, in which the vesicles were swollen, a glucose-water solution ($\sim 5\%$ w/w), with 500 kDa molecular weight dextran in various concentrations up to 6% w/w added to increase the fluid viscosity, was used. The viscosity contrast different from unity was achieved by gentle centrifugation to washing out the outer medium and replacing it by a sucrose-glucose-dextran-water solution of

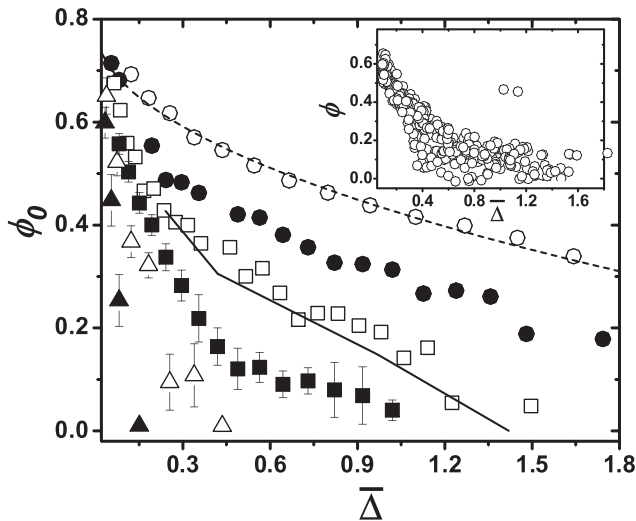


FIG. 1. ϕ_0 as a function of $\bar{\Delta}$ for several values of ϵ : open circles—1, full circles—2.6, open squares—4.2, full squares—5.3, open triangles—6.6, full triangles—9.1. Dashed line is theoretical expression $\phi_0 \approx \pi/4 - 0.354\bar{\Delta}^{1/2}$ taken from Ref. [2]. Solid line is numerical simulations at $\epsilon = 3.7$ [6]. The inset: ϕ vs $\bar{\Delta}$ at $\epsilon = 5.3$.

the same osmolarity and density to control the outer fluid viscosity and to compensate for a gravity. The experiments were conducted at temperatures between 22 and 24 °C to keep the membrane in a liquid state. The viscosity measurements of every solution were carried out on a viscometer Vilastic-3.

A dilute solution of deflated vesicles was driven through a microchannel by a microsyringe pump at a constant flow rate. The profile of the horizontal velocity was measured and was similar to that reported in Ref. [10]. The measurements of vesicle dynamics were performed at a distance between about 5 and 45 μm from the wall. The deviation of the shear rate from a constant was at the most $\pm 5\%$ on the vesicle size. A drift velocity due to the lift force was at least 3 orders of magnitude smaller than a vesicle horizontal velocity, and the resulting drift during an experimental time ($\sim 3 \mu\text{m}$) was smaller than due to all other experimental factors.

We conducted two types of measurements of the vesicle dynamics: the experiments on the vesicle orientation in a tank-treading regime at every $\epsilon < \epsilon_c$ were carried out in a laboratory frame (see Figs. 1–3), and the experiments in a tumbling regime were conducted in a moving frame with a velocity of a single captured vesicle to collect statistics in time (see Figs. 4 and 5). The latter measurements were done by translating the channel by means of a motorized stage with the velocity of the captured vesicle and simultaneous grabbing images at a rate of 25 fps. A single vesicle could be traced up to 40 sec providing up to 1000 measurements to collect statistics in time for a vesicle.

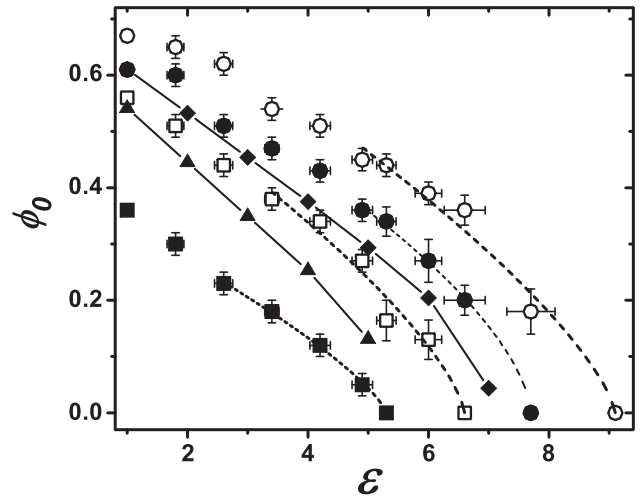


FIG. 2. The same data as in Fig. 1 presented in the coordinates ϕ_0 and ϵ at different values of $\bar{\Delta}$: open circles—0.15, full circles—0.24, open squares—0.42, full squares—1.42. Rhombus and triangles connected by solid lines are numerical simulations at $\bar{\Delta} = 0.34$ and $\bar{\Delta} = 0.58$, respectively [6]. Dashed lines are fits by $\phi_0 = a|\epsilon - \epsilon_c|^b$ with $a = 0.17 \pm 0.03$, $b = 0.73 \pm 0.13$ —open circles; $a = 0.19 \pm 0.01$, $b = 0.63 \pm 0.04$ —full circles; $a = 0.17 \pm 0.02$, $b = 0.72 \pm 0.12$ —open squares; $a = 0.11 \pm 0.03$, $b = 0.76 \pm 0.03$ —full squares.

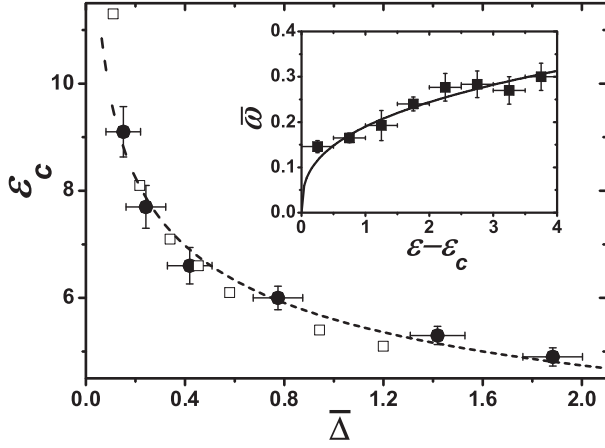


FIG. 3. ϵ_c vs $\bar{\Delta}$. Full circles with error bars are the experimental data, open squares are numerical simulations [6], and dashed line is the fit $\epsilon_c = (5.6 \pm 0.1)\bar{\Delta}^{-0.24 \pm 0.02}$. The inset: $\bar{\omega}$ vs $\epsilon - \epsilon_c$ in tumbling motion regime. Solid line is the fit by $\bar{\omega} = a(\epsilon - \epsilon_c)^b$ with $a = 0.19 \pm 0.01$ and $b = 0.36 \pm 0.05$.

The inclination angle, ϕ , between the flow direction and the long axis of an elliptical approximation of a vesicle image, and the excess area of a vesicle moving at a given shear rate, were defined via image analysis in terms of shape recognition using MATLAB IP toolbox [10]. Only the systematic excess area, $\bar{\Delta}$, the elliptical part of the surface area, can be measured experimentally, since the part of the

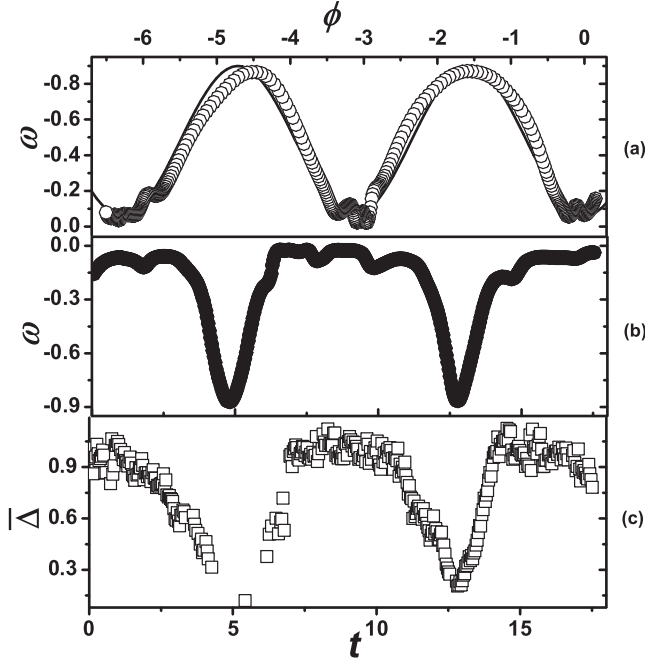


FIG. 4. (a) ω as a function of ϕ in tumbling motion; solid line is the fit $\omega = A + B \cos(2\phi)$ with the parameters $A = -0.48$ and $B = 0.42$. (b) ω as a function of time for the same vesicle. (c) $\bar{\Delta}$, as a function of time for the same vesicle. The parameters of the vesicle and the flow are: $R = 4.7 \mu\text{m}$, $\bar{\Delta}_{\text{max}} = 1.1$, $\epsilon = 6$, $\dot{\gamma} = 1.8 \text{ s}^{-1}$.

excess area stored in thermally induced undulations of the vesicle membrane is below the optical resolution. So we use $\bar{\Delta}$ instead of Δ . Besides, since we have measured ϕ at sufficiently large shear rates ($\chi_T \equiv \dot{\gamma} \eta_{\text{out}} R^3 / k_B T \gg 1$), the thermally induced undulations are negligible, and $\bar{\Delta} \approx \Delta$ [2,10].

Dependence of the mean inclination angle averaged over an ensemble, ϕ_0 , on $\bar{\Delta}$ for different values of ϵ are presented in Fig. 1 (here only part of the data is shown). The measurements were conducted for vesicles with radii in the range $R = 3\text{--}14 \mu\text{m}$, shear rates $\dot{\gamma} = 3\text{--}12 \text{ s}^{-1}$, and viscosities of inner and outer solutions in the ranges $\eta_{\text{in}} = 9\text{--}12 \text{ cP}$ and $\eta_{\text{out}} = 1.3\text{--}5 \text{ cP}$, respectively. Then $\chi_T \gg 1$ and it varies in the range between about 30 and 3000. The data for $\epsilon = 5.3$ shown in the inset in Fig. 1 exhibit a rather large scatter of ϕ . It appears mostly due to fluctuations in ϵ and less due to thermal fluctuations. For each curve with a specific value of ϵ up to 500 vesicles were investigated. Then the data were divided into boxes that correspond to certain values of $\bar{\Delta}$, and averaged over each box. In such a way the dependence of ϕ_0 on $\bar{\Delta}$ averaged over ensembles was obtained for each ϵ . The dashed line is the theoretical curve for $\epsilon = 1$ without any fitting parameter [2], and the solid line is the result of the numerical calculations for $\epsilon = 3.7$ [6].

Figure 2 shows the same data for ϕ_0 presented as a function of ϵ for 4 values of $\bar{\Delta}$ that differ up to 10 times. All curves show close to the transition to the tumbling a

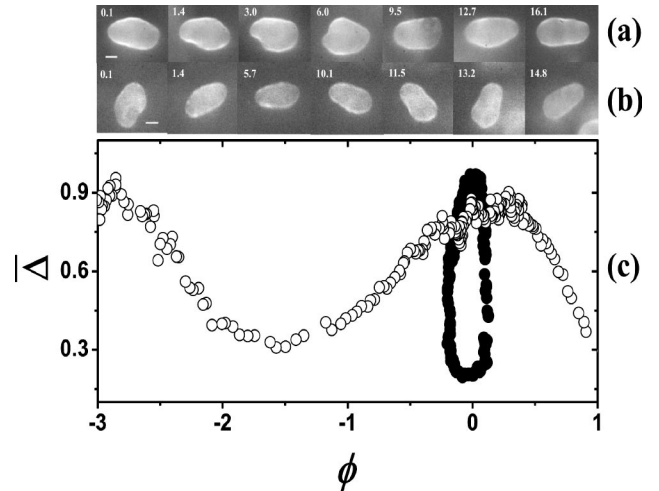


FIG. 5. (a) Time series of snapshots of a vesicle in a trembling motion with shape deformation oscillations. The parameters of the vesicle and flow are: $R = 8.4 \mu\text{m}$, $\bar{\Delta}_{\text{max}} = 1.0$, $\epsilon = 6$, and $\dot{\gamma} = 1.8 \text{ s}^{-1}$. (b) Time series of snapshots of a vesicle in a tumbling motion with strong shape deformations. The parameters of the vesicle and flow are: $R = 6.6 \mu\text{m}$, $\bar{\Delta}_{\text{max}} = 0.9$, $\epsilon = 8.4$, and $\dot{\gamma} = 1.7 \text{ s}^{-1}$. Numbers in the left corners of each image are elapsing normalized, $t\dot{\gamma}$, and the scale bars are $5 \mu\text{m}$. (c) $\bar{\Delta}$ as a function of ϕ : open circles are the data for the vesicle in (b), and full circles are the data for the vesicle in (a).

functional dependence as $\phi \propto (\epsilon_c - \epsilon)^b$, where b varies between ~ 0.6 and ~ 0.75 . It differs from $b = 0.5$ predicted by the theory [1,5] but rather close to the numerical simulations [6] shown in Fig. 2. The transition indeed occurs via a saddle-node bifurcation [1,3,5]. And finally, the critical values of the viscosity contrast, ϵ_c , obtained from the data presented in Figs. 1 and 2, are shown in Fig. 3 as a function of $\bar{\Delta}$ together with the results of the numerical calculations [6]. The dashed line is the fit to the data $\epsilon_c = (5.6 \pm 0.1)\bar{\Delta}^{-0.24 \pm 0.02}$. The agreement is rather impressive, particularly if one recalls that the simulations are based on the model in the regime of weakly deformable vesicles, $\chi < 1$, whereas the experimental data were taken at $\chi \gg 1$.

In the tumbling motion regime we found, to our surprise, two types of a flipping motion. At moderate values of $\chi < 10$, the expected tumbling with a vesicle axis rotating in respect to the flow direction is observed, though large shape deformations are accompanied by the flipping [see snapshots in Fig. 5(b)]. In spite of this, the angular dependence of the vesicle reduced angular velocity, $\omega \equiv \dot{\gamma}^{-1}(d\phi/dt)$, is described sufficiently well by Eq. (1). Indeed, in Fig. 4(a) the data on ω versus ϕ are presented together with the fit that is a solution of Eq. (1) with $|A/B| > 1$ as predicted by the theory [1] for the tumbling. The data are taken at $\dot{\gamma} = 1.8 \text{ s}^{-1}$, $\bar{\Delta}_{\max} = 1.1$, $R = 4.7 \mu\text{m}$, $\epsilon = 6$. Here $\bar{\Delta}_{\max}$ is the maximum value of $\bar{\Delta}$ taken from Fig. 4(c). In Figs. 4(b) and 4(c) the data on ω and $\bar{\Delta}$ are presented as a function of time to emphasize a strong correlation between variations of the angular velocity and shape deformations during the tumbling. The similarity in the dynamics of $\bar{\Delta}$ and ω suggests that $\bar{\Delta}$ as a function of ϕ can be described by an equation similar to Eq. (1), as was suggested in Ref. [11]. The data on the tumbling angular velocities, ω , were collected on 40 vesicles over several periods. In the inset in Fig. 3 these data for $\bar{\omega}$ averaged over periods and ensembles are presented as a function of $(\epsilon - \epsilon_c)$ together with the fit. Large error bars and significant scatter are mostly attributed to uncertainty in $(\epsilon - \epsilon_c)$, where $\bar{\Delta}_{\max}$ is taken to define $\epsilon_c(\bar{\Delta})$.

At large $\chi > 10$ and particularly in the close vicinity to the transition, a new type of motion was discovered. A vesicle trembles around $\phi_0 = 0$ with periodical shape deformations [see snapshots in Fig. 5(a)]. The remarkable difference between two types of motion in the unsteady regime is illustrated in Fig. 5(c), where $\bar{\Delta}$ as a function of ϕ for both types of motion is presented. In Fig. 5(c) full circles show the data taken for the vesicle, which dynamics are illustrated by the snapshots in Fig. 5(a). The parameters of this vesicle and the flow are: $R = 8.4 \mu\text{m}$, $\bar{\Delta}_{\max} = 1.0$, $\epsilon = 6$, and $\dot{\gamma} = 1.8 \text{ s}^{-1}$ that gives $\chi \approx 22$ [at $\kappa \approx 10^{-12} \text{ erg}$ taken from literature, see, e.g., Ref. [15]]. Open circles in Fig. 5(c) show the data taken for the vesicle, which dynamics are illustrated by the snapshots in Fig. 5(b). The parameters of this vesicle and the flow are: $R = 6.6 \mu\text{m}$, $\bar{\Delta}_{\max} = 0.9$, $\epsilon = 8.4$, and $\dot{\gamma} = 1.7 \text{ s}^{-1}$ that

leads to $\chi \approx 6$. One notes that variations in $\bar{\Delta}$ in both cases are large and comparable but the variations in ϕ for these two types of motion differ both qualitatively and quantitatively by an order of magnitude [Fig. 5(c)].

To conclude, the experimental results on the tank-treading-tumbling transition $\epsilon_c(\bar{\Delta})$ in dynamics of a vesicle subjected to a shear flow show a surprising agreement with both theoretical predictions based on a simple fixed shape vesicle model [1] and numerical simulations [6], in spite of the fact that they consider either nondeformable or a weakly deformable vesicle, whereas the experiments deal with a strongly deformable one. The algebraic decay of ϕ_0 in the steady tank-treading motion for various values of $\bar{\Delta}$ is found in agreement with numerical simulation [6] but differs from $\sqrt{\epsilon_c - \bar{\epsilon}}$ dependence predicted by the theory [1,5]. Strong correlation between variations of the angular velocity and large shape deformations during the tumbling suggests that the new model [11] rather than the former ones [1,3] should appropriately describe these dynamics. But the most unexpected finding is the observation of a new type of unsteady motion at large degree of vesicle deformability, defined by $\chi \gg 1$: the vesicle trembles around the flow direction, while the vesicle shape strongly oscillates.

We thank V. Lebedev for helpful remarks and E. Segre for help in software support. This work is partially supported by grants from Israel Science Foundation, Binational US-Israel Foundation, and by the Minerva Center for Nonlinear Physics of Complex Systems.

-
- [1] S. R. Keller and R. Skalak, *J. Fluid Mech.* **120**, 27 (1982).
 - [2] U. Seifert, *Eur. Phys. J. B* **8**, 405 (1999).
 - [3] F. Rioual, T. Biben, and C. Misbah, *Phys. Rev. E* **69**, 061914 (2004).
 - [4] M. Kraus, W. Wintz, U. Seifert, and R. Lipowsky, *Phys. Rev. Lett.* **77**, 3685 (1996).
 - [5] T. Biben and C. Misbah, *Phys. Rev. E* **67**, 031908 (2003).
 - [6] J. Beaucourt, F. Rioual, T. Seon, T. Biben, and C. Misbah, *Phys. Rev. E* **69**, 011906 (2004).
 - [7] K. de Haas, C. Bloom, D. van den Ende, M. Duits, and J. Mellema, *Phys. Rev. E* **56**, 7132 (1997).
 - [8] M. Abkarian, C. Lartigue, and A. Viallat, *Phys. Rev. Lett.* **88**, 068103 (2002); M. Abkarian and A. Viallat, *Biophys. J.* **89**, 1055 (2005).
 - [9] V. Vitkova, M. Mader, T. Biben, and T. Podgorski, *J. Optoelectr. Adv. Mater.* **7**, 261 (2005).
 - [10] V. Kantsler and V. Steinberg, *Phys. Rev. Lett.* **95**, 258101 (2005).
 - [11] H. Noguchi and G. Gompper, *Phys. Rev. Lett.* **93**, 258102 (2004).
 - [12] G. B. Jeffery, *Proc. R. Soc. A* **102**, 161 (1922).
 - [13] Y. N. Xia and G. M. Whitesides, *Annu. Rev. Mater. Sci.* **28**, 153 (1998).
 - [14] M. I. Angelova, S. Soleau, P. Meleard, J.-F. Faucon, and P. Bothorel, *Prog. Colloid Polym. Sci.* **89**, 127 (1992).
 - [15] W. Rawicz *et al.*, *Biophys. J.* **79**, 328 (2000).